Pharm Res
DOI 10.1007/s11095-017-2225-0

RESEARCH PAPER

# Chitooligosaccharides Modified Reduction-Sensitive Liposomes: Enhanced Cytoplasmic Drug Delivery and Osteosarcomas-Tumor Inhibition in Animal Models

Xuelei Yin[1] • Yingying Chi[1] • Chuanyou Guo[2] • Shuaishuai Feng[1] • Jinhu Liu[1] • Kaoxiang Sun[1] • Zimei Wu[1,3]

Received: 26 February 2017 / Accepted: 28 June 2017


## ABSTRACT

***Purpose*** To investigate the potential of a reduction-sensitive and fusogenic liposomes, enabled by surface-coating with chotooligosaccharides (COS) via a disulfide linker, for tumor-targeted cytoplasmic drug delivery.

***Methods*** COS (MW2000-5000) were chemically tethered onto the liposomes through a disulfide linker (-SS-) to cholesterol (Chol). Doxorubicin (DOX) was actively loaded in the liposomes. Their reduction-sensitivities, cellular uptake, cytotoxicity, pharmacokinetics and antitumor efficacy were investigated.

***Results*** The Chol-SS-COS/DOX liposomes (100 nm) had zeta potential of 33.9 mV and high drug loading (13% *w*/w). The liposomes were stable with minimal drug leakage under physiological conditions but destabilized in the presence of reducing agents, dithiothreitol (DTT) or glutathione (GSH) at 10 mM, the cytosolic level. MTT assay revealed that the cationic Chol-SS-COS/DOX liposomes had higher cytotoxicity to MG63-osteosarcoma cells than non-reduction sensitive liposome (Chol-COS/DOX). Flow cytometry and confocal microscopy revealed that Chol-SS-COS/DOX internalized more efficiently than Chol-COS/DOX with more content to cytoplasm whereas Chol-COS/DOX located around the cell membrane. Chol-SS-COS/DOX preferentially internalized into MG63 cancer cell over LO2 normal liver cells. In rats both liposomes produced a prolonged half-life of DOX by 4 - 5.5 fold ($p < 0.001$) compared with the DOX solution. Chol-SS-COS/DOX exhibited strong inhibitory effect on tumor growth in MG63 cell-bearing nude mice ($n = 6$), and extended animal survival rate.

***Conclusions*** Reduction-responsive Chol-SS-COS liposomes may be an excellent platform for cytoplasmic delivery of anticancer drugs. Conjugation of liposomes with COS enhanced tumor cell uptake, antitumor effect and survival rate in animal models.

**KEY WORDS** Chotooligosaccharides (COS) · Cationic liposomes · Reduction-sensitivity · Cytoplasmic delivery · Tumor-suppression · Survival rate

## ABBREVIATIONS

| | |
|---|---|
| Chol | Cholesterol |
| COS | Chitooligosaccharides |
| DCC | N,N′-dicyclohexylcarbodiimide |
| CLSM | Confocal laser scanning microscopy |
| DOX | Doxorubicin |
| DTOP | 3,3′-dithiodipropionic acid |
| DL | Drug loading |
| DLS | Dynamic light scattering |
| DMAP | 4-Dimethylaminopyridine |
| DMEM | Dulbecco's Modified Eagle Medium |
| DTOP | 3,3′-Dithiodipropionic acid |
| DTT | Dithiothreitol |
| EDC | 1-Ethyl-3-(3-dimethylaminopropyl) carbodiimide hydrochloride |
| EE | Entrapment efficiency |
| EPR | Enhanced permeability and retention |
| FBS | Fetal bovine serum |
| FCM | Flow cytometry |
| FTIR | Fourier transform infrared |

✉ Kaoxiang Sun
sunkaoxiang@luye.cn

✉ Zimei Wu
z.wu@auckland.ac.nz

[1] School of Pharmacy, Key Laboratory of Molecular Pharmacology and Drug Evaluation, (Yantai University), Ministry of Education, Collaborative Innovation Center of Advanced Drug Delivery System and Biotech Drugs in Universities of Shandong, Yantai University, Yantai 264005, People's Republic of China

[2] Department of Bone Joint, Qingdao Municipal Hospital, Qingdao, Shandong Province 266011, China

[3] School of Pharmacy, University of Auckland, Auckland 1142, New Zealand

Published online: 19 July 2017

| | |
|---|---|
| GSH | Glutathione |
| MTT | 3-(4, 5-dimethylthiazol-2-yl)-2, 5-diphenyl tetrazolium bromide |
| NHS | N-hydroxysuccinimide |
| PDI | Polydispersity index |
| PEG | Polyethylene glycol |
| RES | Reticuloendothelial system |
| SA | Succinic anhydride |
| SPC | Soybean phosphatidylcholine |
| TLC | Thin-layer chromatography |

## INTRODUCTION

Nano-liposomes are perceived as most biocompatible and biodegradable vesicular carriers for tumor-targeted drug delivery [1–3] through the enhanced permeability and retention (EPR) effect [4]. Recent effort has been devoted to confer liposomes with stimuli-responsiveness [5] to exploit the special features of tumors such as redox potential [3, 6, 7] tumor acidity [8, 9] and special enzyme [10] as stimuli to selectively trigger drug release at the target. In particular, disulfide bond has been widely used in the design of redox sensitivity nanocarriers by exploiting the glutathione (GSH) in cancer cells as a stimulus [3, 6, 7]. The concentration of GSH inside cancer cells is significantly higher (up to 10 mM) than the extracellular level (2-10 μM) [3] or in the normal cells (0.1 mM) [5]. The presence of pendant thiol group (-SH) in GSH makes it a powerful reducing agent and can intracellularly triggered cleavage of disulfide bonds (-SS-).

To exert EPR effect, liposomes (and drug) need to stay in systemic circulation for a sufficient prolonged period of time [11]. This can is achieved by coating the carriers with a hydrophilic polymer which sterically hinders opsonization and thus preventing destruction by reticuloendothelial system (RES) [12, 13]. The gold-standard polymer to date is polyethylene glycols (PEG) [11, 14]. However, recent research showed major drawbacks of PEGylation, including reduced cellular uptake and slow release from endosomes [15, 16], and induction of anti-PEG IgM antibodies which results in accelerated blood clearance (ABC) phenomenon following repeated administration [17]. Alternative polymers poly [N-(2-hydroxypropyl) methacrylamide] (HPMA), poly(vinylpyrrolidone) (PVP) [18], and chitosan derivatives [19, 20] have been explored to prolong blood circulation of liposomes.

Chitosan, a class of naturally occurring polysaccharides consisting of β-(1→4)-linked d-glucosamine (deacetylated unit) and *N*-acetyl-d-glucosamine (acetylated unit), have been popular polymers for drug delivery due to their excellent biocompatibility, biodegradability, and mucoadhesiveness [21], and biological activities, including antitumoral, antimicrobial, and antiviral activities [21, 22]. The amphiphilic chitosan derivatives have recently been widely used to construct or surface-modify nanocarriers for targeted drug delivery [21, 23, 24]. N-palmitoyl chitosan (MW 65 kDa) modified liposomxes increased systemic circulation of free drug docetaxel by approximately 5.5 times, although not as significant as PEGylation (10 times) [20]. More recently, glycol-chitosan coated liposomes were demonstrated to have pH-sensitivity due to the protonation of -$NH_2$ groups which rendered positive charge to liposomes at tumor extracellular low pH (6.5). This charge effect enhanced cellular uptake of liposomes and thus antitumor efficacy compared with non-coated liposome ($p < 0.05$) [25].

Chitooligosaccharides (COS) is a class of hydrolytic products of chitosan. The hydrophilic backbone and low degree of polymerization (n ≈ 2-20) renders COS high water-solubility [26] and wider biological activities than the large molecular chitosan at cellular and molecular levels. The free amino groups allow interactions between COS and the cells consequently increasing cell adhesion. Moreover, their widely reported anti-angiogenesis and radical scavenging efficacy [26–28] of COS, partially by induction of GSH level in the cells [29], made them excellent candidate polymer for modification of tumor-targeted liposomes.

In this work, we aimed to prepare liposomes with COS conjugated on the surface of liposomes via a disulfide linker (-SS-). The liposomes were designed to be stable under normal physiological conditions; the cell adhesive property of COS will facilitate internalization of liposomes into tumor cells. Upon entering cells, the cleavage of disulfide bond by the intracellular GSH would allow destabilization of the vesicles, facilitating rapid release of the payload in cytoplasm. Doxorubicin (DOX) was used as a model drug as well as a fluorescent marker. The *in vitro* cellular uptake and cytotoxicity of liposomes were studied in human osteosarcoma cell lines (MG63). Osteosarcoma is a heterogeneous malignant bone tumor that has the ability to produce osteoid or immature bone, most prevalent in children and young adults. Non-reducible Chol-COS coated liposomes were prepared and used as controls for the proof of concepts. In this paper, we report the synthesis of cholesterol derivatives, Chol-SS-COOH and Chol-COOH, that were used to conjugate COS on liposomes.

## MATERIALS AND METHODS

### Materials

Soybean phosphatidylcholine (SPC), cholesterol (Chol), doxorubicin hydrochloride (DOX·HCl) and chemical agents, 3,3′-dithiodipropionic acid (DTOP), succinic anhydride (SA), 1-ethyl-3-(3-dimethylaminopropyl) carbodiimide hydrochloride (EDC·HCl), N-hydroxysuccinimide (NHS), 4-dimethylaminopyridine (DMAP), and glutathione (GSH) were

all purchased from Aladdin (Shanghai, China). Chitooligosaccharides (MW 2000-5000 and degree of deacetylation 75%) were purchased by Fengan Bio-Pharmaceutical Co. (Zhejiang, China).

MG-63 cell line was purchased from BeNa Cell Collection (Beijing, China), and LO2 cells were gift from Medicine and Pharmacy Research Center, Binzhou Medical University. The chemical agents, 3-(4, 5-dimethylthiazol-2-yl)-2, 5-diphenyl tetrazolium bromide (MTT) and Hoechst 33,342 were obtained from Sigma–Aldrich (USA) while Dulbecco's Modified Eagle Medium (DMEM), Roswell Park Memorial Institute (RPMI) 1640 Medium, and fetal bovine serum (FBS) were purchased from Hyclone (LA, USA). All other chemicals were of analytical reagent grade and used without further purification.

Both Sprague-Dawley (SD) male rats, for pharmacokinetic study, and male BALB/c nude mice, for anti-tumour efficacy, were purchased from Beijing Vital River Laboratory Animal Technology Co., Ltd. and treated according to the protocols prior to use. Animal studies were approved by the Experimental Animals Administrative Committee of Yantai University.

## Synthesis of Chol-SS-COOH and Chol-COOH

To coat COS on liposomes, Chol-SS-COOH and Chol-COOH were first synthesized (Scheme 1) before used for liposome preparation.

Chol-SS-COOH was synthesized using a DCC/DMAP coupling method. Briefly, 3,3′-dithiodipropionic acid (DTOP) dissolved in dimethyl sulfoxide (DMSO) was added to a solution of N,N′-dicyclohexylcarbodiimide (DCC) and 4-dimethylaminopyridine (DMAP) in DMSO under $N_2$ atmosphere. Upon complete dissolution, a certain amount of cholesterol was added dropwise at room temperature with constant stirring. The progress of reaction was monitored by thin-layer chromatography (TLC) with a mobile phase of methylbenzene/ethyl acetate 1:1, *v*/v. After 24 h reaction was complete and excess deionized water was added into the above solution to allow unreacted DCC and the by-product 1,3-dicyclohexylurea to precipitate. The precipitate was removed by filtration while the filtrate containing Chol-SS-COOH was dialyzed against deionized water using a dialysis bag of MWCO ≈ 2000 Da and lyophilized to obtain Chol-SS-COOH. The crude product was re-dissolved in ethyl acetate before loaded on a silica gel column for further purification. The column was washed with mixture of petroleum ether and ethyl acetate (1:10, *v*/v). The eluted product was dried under reduced pressure to obtain pure Chol-SS-COOH.

The Chol-COOH was synthesized successfully according to the method reported by Yu *et al.* [30]. Briefly, cholesterol and succinic anhydride (SA) were dissolved in pyridine and kept for 24 h with constant stirring at room temperature. Then, deionized water was added to the above solution. The produced precipitate was obtained by filtration and dried. The crude product was recrystallized in acetone to obtain the white powder, Chol-COOH.

The structures of the compounds, Chol-SS-COOH and Chol-COOH, were characterized by nuclear magnetic resonance spectrometer ($^1$H NMR, Bruker ARX-400, Switzerland) using deuterated DMSO-*d6* as the solvent.

## Preparation of DOX-loaded liposomes conjugated with COS

The liposomes, Chol-SS-COS-L and Chol-COS-L, were prepared by ethanol injection method followed by conjugation with COS. Briefly, SPC and Chol-SS-COOH or Chol-COOH (molar ratio 10:1.4, total lipids about 30 mg) were added in 1 ml ethanol and sonicated for 10 min. The lipid solution was added into 10 ml PBS (pH 7.4) slowly dropwise with stirring 1 h to obtain a liposomes colloidal suspension. COS polymer (30 mg) was added to the above liposomes, and tethered through a EDC/NHS coupling reaction by which an amide bond was formed between the free -COOH groups of liposomes and free -$NH_2$ of COS [25]. Briefly, the coupling agents, EDC (4.6 mg) and NHS (2.7 mg) were added to the liposomes suspension and kept under stirring at room

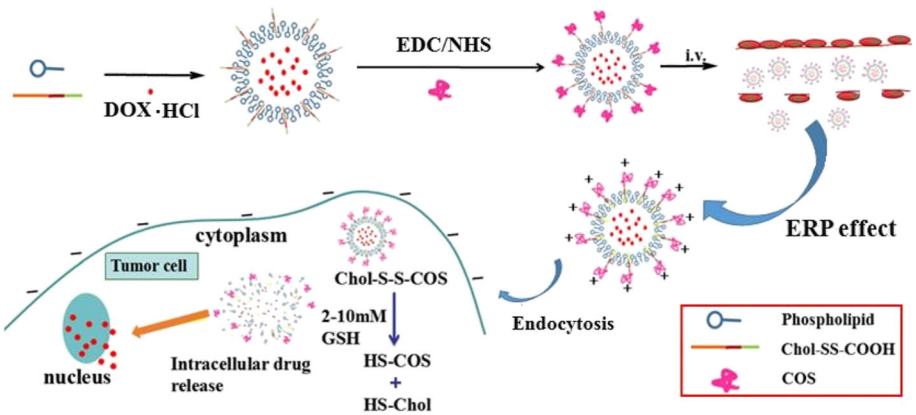


**Scheme 1** Synthesis of a simple and less expensive liposome system as a potential tumor targeted drug delivery platform with three targeting features united: long circulation, fusogenicity, and glutathione (GSH)-responsiveness.

temperature overnight, allowing COS to be conjugated with liposomes.

Conjugation was confirmed by Fourier transform infrared (FTIR) spectrometer (PerkinElmer Frontier, UK).

DOX was loaded into the liposomes using the widely reported ammonium sulfate transmembrane gradient method. The DOX-free liposomes was prepared as described above with 120 mM $(NH_4)_2SO_4$ during film hydration. The untrapped external $(NH_4)_2SO_4$ was removed by dialysis against a 10% glucose solution. DOX solution (5 mg/ml) was added to the above liposomes solution and incubated at 40 ▫C for 3 h while stirring and protected from light. The free DOX was removed from the DOX-loaded liposomes by dialysis.

### Characterization of liposomes

The particle size and zeta-potential of DOX-loaded liposomes were measured by dynamic light scattering (DLS, Malvern Instruments Ltd., UK) after dispersed in PBS (pH 7.4). The pH effect on zeta-potential was also tested PBS (pH 6, 6.5, and 7). The morphology of liposomes was observed by transmission electron microscope (TEM, JEM-1400, Japan).

To estimate the amount of DOX encapsulated into liposomes, DOX-loaded liposomes were ultra-centrifuged, and freeze-dried before dissolved in ethanol. After centrifuge the DOX concentration in ethanol was measured by fluorescence spectrophotometric measurement (LS-55, Perkin Elmer, USA), with excitation wavelength of 488 nm and an emission wavelength of 593 nm. The linear concentration range of DOX with the fluorescence method was 0.05-1.3 μg/ml ($R^2 > 0.99$). The encapsulation efficiency (EE) and drug loading (DL) was calculated using the following equations:

$$\mathrm{DL}\ (\%) = \frac{\textit{Amount of drug in liposomes}}{\textit{Amount of drug loaded liposomes}} \times 100$$

$$\mathrm{EE}\ (\%) = \frac{\textit{Amount of drug in liposomes}}{\textit{Total amount of feeding drug}} \times 100$$

### Reduction-sensitivity of DOX-loaded Chol-SS-COS liposomes

Reduction-induced destabilization of Chol-SS-COS liposomes was observed by mornitoring the change in size of the liposomes which were suspended in a PBS (0.1 M, pH 7.4) containing 10 mM dithiothreitol (DTT), a reducing agent [8]. The mixture was placed in shaking water bath at 37 ▫C and the change in particle size over 4 h was monitored using a Malvern Zetasizer (DLS). Chol-COS liposomes were used as controls.

In another experiment, to simulate the tumor cellular microenvironments, 1 ml of each liposomal formulation was placed into a dialysis bag (MWCO 10 KDa) and immersed in 30 ml of PBS (10 mM, pH 7.4) containing 10 mM or 20 μM GSH. The samples were maintained at 37 ▫C in a shaking bed. At designed time intervals, aliquots (1 ml) of dialysis medium were taken and replaced with an equivalent volume of fresh medium. The concentrations of released DOX were determined as described above.

### Physical stability of DOX-loaded liposomes

The physical stability of DOX-encapsulated liposomes in PBS (pH 7.4, 10 mM) containing 10% FBS stored at 4 ▫C was monitored by the measurement of particle size using Malvern Zetasizer over 15 days.

### In vitro cytotoxicity assay

MG63 human osteoblast-like osteosarcoma cells and human being's liver cell strain LO2 cells were maintained in 5% $CO_2$ at 37 ▫C in McCoy's 5A medium (FBS 15%, *v*/v) and RPMI-1640 medium (10% FBS, *v*/v), respectively. Both media were supplemented with penicillin-streptomycin (1%, *v*/v). The medium was routinely replaced with fresh medium every day. The cells in logarithmic phase of growth were cryopreserved for cytotoxicity using 3-(4,5-dimethythiazol-2-yl)-2,5-diphenyl tetrazolium bromide (MTT) cell viability assay. Cells were seeded in 96-well plates in the abovementioned medium. The cells were cultured for 24 h hours to allow cells to attach before exposed to COS polymer, non-coated liposomes, free DOX or drug-loaded liposomes. Each of the samples was dispersed in culture medium before adding to the wells. After 24 h or 48 h of incubation, MTT assay was perfosrmed to determine the cytotoxicity. The optical density (OD) of each well was measured at 490 nm using a microplate reader (Spectra Max M2, Molecular Devices, USA). Cell viability was assessed using the following equation:

$$\textit{Cell viability}\ (\%) = \frac{\mathrm{OD}\ \textit{treated}}{\mathrm{OD}\ \textit{control}} \times 100$$

$OD_{treated}$ and $OD_{control}$ represented the OD of treated and untreated (medium) wells, respectively.

### In vitro cellular uptake

To understand the mechanism of liposome-cell interactions and thus cytotoxicity, cellular uptake of Chol-SS-COS/DOX by MG63 and LO2 cells was compared using flow cytometry (FCM) and confocal laser scanning microscopy (CLSM). For both studies, formulations (free DOX, Chol-COS/DOX, Chol-SS-COS/DOX) were dispersed in medium with a final DOX concentration of 20 μg/ml before added into the cells.

For the FCM studies, cells were seeded in 6-well plates ($10^6$/well) in the medium and cultured in 5% CO2 at 37 ▫C, overnight. Then, the cells were treated with different formulations. At different time points, 0, 1, 2, 3, and 4 h, the cells were washed twice with 2 ml of PBS, and detached with trypsin. After centrifuged at 1500 rpm for 5 min, the cells in pellets were re-suspended in 0.5 ml of PBS before analyzed using a FACS Calibur flow cytometer (EPICS XL, Beckman, USA).

For CLSM analysis, cells were seeded onto clean and sterile coverslips placed in a 12-well plates at an initial density of $5 \times 10^5$ cells/well and cultured overnight. Cells were then treated with free DOX, or each of the DOX-containing liposomes, respectively. After incubation at 37 ▫C for 2 h or 4 h, the cells were washed with PBS for three times, fixed with paraformaldehyde solution (4%) for 30 min, stained nucleus with Hoechst 33,342 solution (10 μg/ml) for 10 min before observed under a confocal microscope (TCS SPE, Leica, Germany).

### Pharmacokinetic study

Male SD rats (190 - 210 g) were randomly divided into three treatment groups for pharmacokinetic studies ($n = 3$): free Dox solution, CHOL-COS/DOX, and CHOL-SS-COS/DOX. Drug was administrated intravenously at a dose of 2 mg/kg via tail vein. At the designed time (0.5, 1, 2,4, 6, 8, 24 and 48 h), blood samples were collected from the vena ophthalmica to hepatized tubes. Plasma samples were obtained after centrifuged and drug was extracted by solvent precipitation with chromatographic pure methanol (plasma to methanol ratio 1: 15, *v*/v). After votexing for 10 min, the mixture was centrifuged at 5000 rpm for 20 min and supernatant at fixed volume was dried using Termovap Sample Concentrator (Wuxi Voshin Instruments Co., Ltd., Wuxi, China). The residual was dissolved in 0.2 ml mobile phase and centrifuged and DOX concentration was quantified using high performance liquid chromatography (HPLC) (Agilent Technologies 1260 series, USA). The mobile phase was composed of acetonitrile, methanol and $NaH_2PO_4$ (10 mM, pH 4.2) at volume ratios of 28: 20: 52. The flow rate and column temperature were set at 1 ml/min and 25°C, respectively. The UV absorbance at 254 nm was determined and injection a volume was 20 μl.

Pharmacokinetic parameters were estimated using non-compartmental analysis based on statistical moment theory. Elimination half-life ($t_{1/2}$) was calculated as $t_{1/2} = 0.693/\lambda$, where λ is the slope obtained from the regression of natural log concentration versus time in the terminal phase over the last three measurable data points. The linear trapezoidal rule was used to calculate area under the curve (AUC) and the area under the first moment curve (AUMC) without extrapolation. The mean residence time (MRT) was further obtained as the ratio of AUMC/AUC.

### Anti-tumor efficacy in MG63 tumor bearing nude mice

Male BALB/c nude mice (20 ± 2 g) were used to establish MG63 tumors by subcutaneous inoculation of $1 \times 10^7$ cells in the left hind leg of nude mice. The tumor sizes were closely monitored every second day. Tumor volume was calculated using the formula: $0.5 \times L \times W^2$, with length (L) and width (W) being the largest and smallest diameters of tumors, respectively. Once the tumor size reached approximately 100 $mm^3$ (Day 0), the MG63 tumor bearing mice were randomly divided into four treatment groups ($n = 6$); untreated control (saline), free DOX, CHOL-COS/DOX, and CHOL-SS-COS/DOX. Animals were administered with saline or DOX formulations at 5 mg/kg via the tail veins every 3 days for four times.

### Statistical analysis

All studies were carried out in triplicate. One-way analysis of variance (ANOVA) was used to determine the difference of groups, and data was considered to be significant at p▫0.05.

## RESULTS

### Structural characterization of Chol-SS-COOH and Chol-COOH

$^1$H NMR of Chol-SS-COOH (500 MHZ, DMSO-d6) δ (ppm): 5.57 (d, J = 8.0 Hz, 3H), 5.27 (d, J = 5.2 Hz, 1H), 4.59 (d,J = 4.6 Hz, 1H), 0.95 (s, 3H), 0.90 (d, J = 6.5 Hz, 3H), 0.86 (d, J = 2.4 Hz, 3H), 0.85 (d, J = 2.4 Hz, 3H), 0.66 (s, 3H).

Chol-COOH $^1$H NMR (500 MHZ DMSO-d6) δ (ppm): 12.18 (s, 1H), 5.35 (dd, J = 5.0, 2.0 Hz, 1H), 4.47 (dtd, J = 12.4, 8.6, 4.4 Hz, 1H), 3.32 (s, 4H), 0.98 (s, 3H), 0.90 (d,J = 6.5 Hz,3H), 0.86 (d,J = 2.4 Hz,3H), 0.85 (d,J = 2.3 Hz,3H), 0.66 (s, 3H). The results indicated the formation of the chemical structures.

The yield of Chol-SS-COOH and Chol-COOH was 76.1% and 80.1%, respectively.

### Physico-chemical characteristics of COS conjugated liposomes

Liposomes containing Chol-SS-COOH or Chol-COOH were successfully prepared used for ethanol injection method followed by chemical conjugation with COS. The FTIR spectra of Chol-SS-COOH containing liposomes before (Chol-SS-COOH-L) and after coating with COS (Chol-SS-COS-L) were shown in Fig. 1. The COS-tethered liposomes exhibited an intense peak was observed at 1637.53 $cm^{-1}$ (NH bend

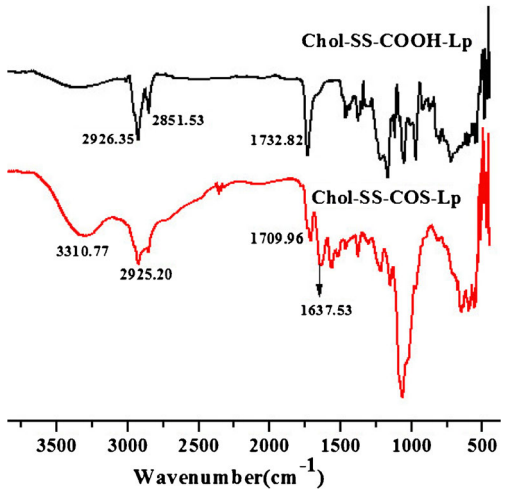


**Fig. 1** FT-IR spectra of Chol-SS-COOH-liposomes (without COS) and Chol-SS-COS liposomes, confirming the conjugation of COS via formation of amide bond (corresponding to the new peak at 1637.53 $cm^{-1}$).

vibration), corresponding to amino bond, confirming effective coupling of amine groups of COS with carboxylic groups (C = O stretch1732.82 cm-1) in the surface of liposomes.

DOX as the most commonly used chemotherapeutic drug was loaded into the liposomes using the ammonium sulfate gradient method with high EE and DL. The particle size and zeta potential of Chol-SS-COS and Chol-COS liposomes are shown in Table I. The average size of nanoparticles was ~70-80 nm with a narrower size distribution (PDI ≒ 0.2) than non-coated liposomes. The particle size of both liposomes increased following conjugation with COS, but this size was suitable to exploit the EPR effect. The ζ potential of the liposomes without COS(CL)was negative, but was turned into positive values after COS was tethered on the surface of both liposomes, confirming the success conjugation of COS which contains $–NH_2$ groups. In addition, TEM images (Fig. 2) show that both Chol-COS and Chol-SS-COS liposomes were spherical. The particle size was smaller than that obtained by DLS, possibly due to shrinkage of the COS polymer layer in a dry state.

## Stability and reduction-sensitivity of liposomes

As shown in Fig. 3, the COS modified liposomes in PBS (pH 7.4, 10 mM) containing 10% FBS was stable for at least 15 days with no significant change in the average size and range (PDI data not shown).

To evaluate the redox-sensitive drug release behavior, the liposomes were placed at 10 mM DTT in PBS (10 mM, pH 7.4), and the size change was measured by DLS. At 10 mM DTT, Chol-SS-COS liposomes, not Chol-COS liposomes, aggregated rapidly, as evidenced with the size of liposomes increasing from 119 ± 1.4 nm to 125 ± 1.5 nm at 2 h and 228.1 ± 4.9 nm after 4 h. At 24 h, the size was increased to 254 ± 3 nm. These results confirmed that Chol-SS-COS liposomes were dissociated in the presence of DTT, most likely due to the cleavage of the -SS- bonds, resulting in detachment of the COS layers. Without the steric repulsion of the COS polymer the uncoated liposomes tend to aggregate or fuse.

## *In vitro* GSH-triggered drug release

The drug release behavior of DOX-loaded liposomes, assessed in PBS (pH 7.4) at 37 ▫C exhibited a sustained-release profile with less than 40% of DOX released after 72 h (Fig. 4). In contrast, the drug release from Chol-SS-COS in presence of 10 mM of GSH (pH 7.4) was fast with >50% of DOX released within the first 10 h whearas in the absence of or low concentration of GSH (20 μM), the accumulative release of DOX was both lower than 40%. For Chol-COS liposomes, the drug release rate was lower than 20% with slight increase in the presence of GSH (<30%). In general, DOX release from Chol-SS-COS-L were faster than from Chol-COS liposomes.

## *In vitro* cytotoxicity assay

The cytotoxic effects of blank liposomes on MG63 and LO2 using MTT assay were shown in Fig. 5A and B, respectively. Compared with the medium treated cells, the cell viability remained more than 85% at all the tested concentration up to 100 μg/ml after 48 h incubation, suggesting that empty liposomes were nontoxic. Similarly, COS polymer itself had no cytotoxicity toward the two cell lines, consistent with the wide report in the literature.

To evaluate the cytotoxicity of various DOX formulations, cells were treated with different DOX formulations at a concentration range of 0.001 to 10 μg/ml. After 24 h incubation, the cell proliferation was measured with MTT assay. All

**Table I** The physicochemical characteristics of non-coated liposomes (containing Chol-SS-COOH) and COS coated liposomes. Data are mean ± SD, $n = 3$

| Liposomes | Particle size (nm) | PDI | zeta potential (mV) | DL (% *w/w*) | EE (% *w/w*) |
|---|---|---|---|---|---|
| Chol-SS-COOH-L | 74.17 ± 2.22 | 0.279 ± 0.003 | −6.52 ± 1.86 | 15.2 ± 0.87 | 96.1 ± 4.99 |
| Chol-SS-COS/DOX | 105.7 ± 0.42 | 0.197 ± 0.008 | 33.9 ± 0.737 | 12.9 ± 2.34 | 85.4 ± 1.36 |
| Chol-COS/DOX | 81.27 ± 1.13 | 0.216 ± 0.007 | 37.7 ± 1.33 | 13.3 ± 2.97 | 91.3 ± 26.5 |

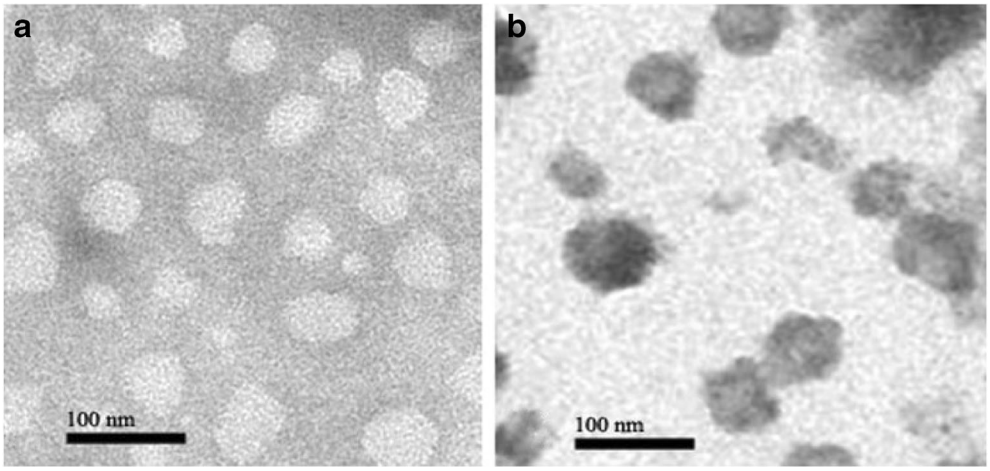


**Fig. 2** Transmission electron microscopy (TEM) images of conventional liposomes with no COS coating (**a**), and Chol-SS-COS-L, similar to Chol-COS-L (**b**).

formulations showed DOX dose-dependent toxicity to both cells (Figs. 5C and D). The order of cytotoxicity to MG63 of the formulations was ranked as: free DOX ≒ Chol-SS-COS/DOX-L ≒ Chol-COS/DOX-L, as shown by the half inhibitory concentrations ($IC_{50}$) ($p < 0.01$). Moreover, significantly higher cytotoxicity against cancerous MG63 cells than to LO2 liver cells were observed with all formulations at all concentration levels ($p < 0.01$).

### *In vitro* cellular uptake

The kinetics of cellular uptake of Chol-SS-COS/DOX-L and Chol-COS/DOX-L compared with free DOX by MG63 and LO2 cells was quantified using flow cytometry (Fig. 6). The cellular uptake of all formulations by both cell types increased in a time-dependent manner within the 4 h, and the cellular fluorescence intensity being ranked in the same order: free DOX > Chol-SS-COS/DOX-L > Chol-COS/DOX-L. Moreover, the mean fluorescence intensity of DOX in MG63 cells was significantly higher than that in LO2 cells, particularly Chol-SS-COS/DOX-L, suggesting their selectivity for tumor cells.

The cellular uptake of different formulations was further visually observed in MG63 and LO2 cells with confocal laser scanning microscopy (Figs. 6 and 7). Similar to the flow cytometry, the fluorescence intensity of DOX enhanced over time but the signals in MG63 were much stronger than in LO2 cells. The formulations were ranked in the same order as per the fluorescence intensity in the cells as ranked in the flow cytometry. Interestingly, DOX was seen mainly distributed in cellular nuclei of MG63 cells following the treatment with free DOX, but mainly distributed in cytoplasm, and in particular, surrounding the nuclear areas following the treatment with Chol-SS-COS/DOX-L.

### Pharmacokinetics

Following i.v. injection of DOX solution, the plasma drug concentration in rats dropped rapidly with only a minimal concentration was observed in the chromatograms at 4 h (< 50 ng/ml). In contrast, the drug concentrations from both liposomes were measurable after 8 h (Fig. 8). Compared with the free DOX, the AUC of liposomal formulations were increased by approximately 3-fold

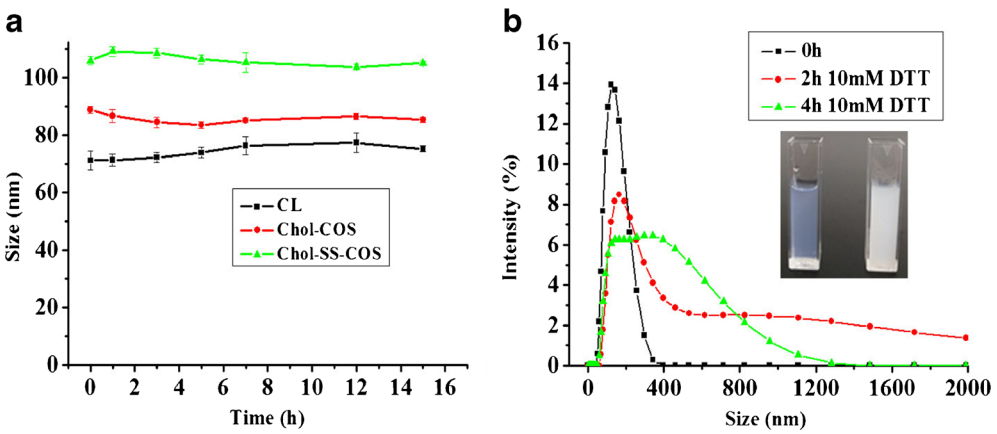


**Fig. 3** (**A**) Stability of the particle size of DOX-encapsulated liposomes in PBS (pH 7.4, 10 mM) containing 10% FBS stored at 4 □C over 15 days ($n = 3$). (**B**) Change in the particle size of Chol-SS-COS liposomes in PBS (pH 7.4) after incubation for 2 h or 4 h in 10 mM DTT solutions at 37□C. Chol-COS liposomes did not show significant change.

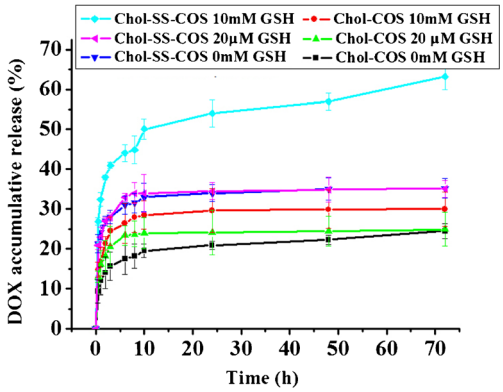


**Fig. 4** DOX release profiles from Chol-COS-L and Chol-SS-COS-L in the absence or presence of GSH at concentrations of 20 $\mu$M (extracellular level) or 10 mM (intracellular level) in PBS (10 mM, pH 7.4) at 37 □C ($n = 3$).

while $T_{1/2}$ increased by 4.0 and 5.6-fold for Chol-SS-COS/DOX-L and Chol-COS/DOX-L, respectively ($p < 0.01$) (Table II). Maximum drug concentration ($C_{max}$) as observed at 0.5 h were similar for the two liposome groups but significantly higher than the free DOX. Apart from a significant longer $T_{1/2}$ ($p < 0.05$), the AUC and MRT values of the Chol-COS/DOX-L group were higher than those of the Chol-SS-COS/DOX-L group, but the differences were not statistically significant ($p > 0.05$).

### *Anit*-tumor efficacy and survival rate

*In* MG63 tumor-bearing nude mice, the tumor size of untreated group (injected with saline only) increased rapidly over time (Fig. 9 A). Intravenous injection of DOX solution every 3 days for four times (Day 0 - 12) resulted in significant inhibitory effect on tumor growth ($p < 0.01$). However, unfortunately animal death was found from Day 14 with only 50% of the animals survived during the experiment (Fig. 9 B). In comparison, the tumor growth rate was remarkably suppressed with Chol-COS/DOX and particularly Chol-SS-COS/DOX liposomes. Furthermore, Chol-SS-COS/DOX liposomes demonstrated the most distinguished effect on extending survival of MG63-bearing mice (Fig. 9B).

## DISCUSSION

Targeted drug delivery with liposomes has played a major role in improving cancer chemotherapy. Recent effort has been made to confer liposomes long circulation property, fusogenicity, and tumor microenvironment-responsiveness to enhance the EPR effect, cellular uptake and cytoplasmic delivery efficiency, respectively. In this study, a simple and less expensive liposome system by tethering

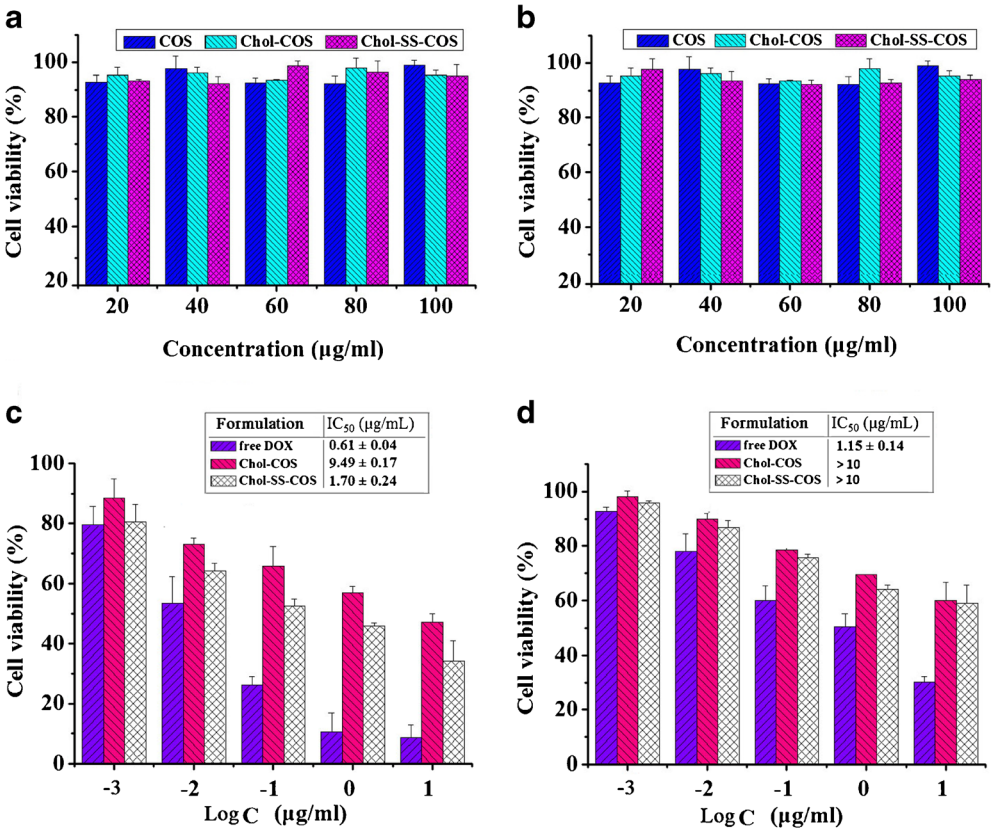


**Fig. 5** *In vitro* cell viability of blank liposomes at different concentrations of lipids against MG63 (**A**) and LO2 (**B**) following 48 h incubation. *In vitro* cytotoxicity of free DOX, Chol-COS/DOX-L and Chol-SS-COS/DOX-L against MG63 (**C**) and LO2 (**D**) cells following 24 h exposure, showing for all DOX formulations had higher cytotoxicity against cancerous MG63 cells than to normal liver cells LO2 ($p < 0.01$). The cytotoxicity was measured by MTT assay, and data are mean ± SD ($n = 6$).

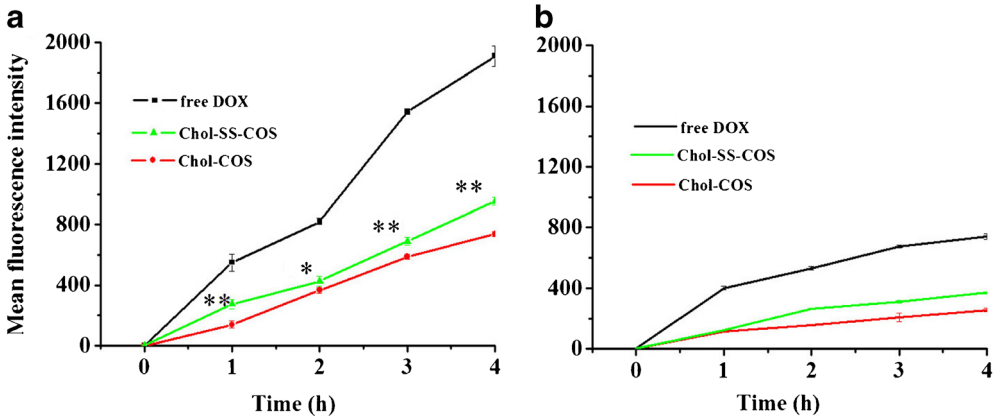


**Fig. 6** Flow cytometry analyses of MG63 (**A**) and LO2 (**B**) cells incubated with different formulations, showing the fluorescence intensity of DOX in the cells increasing over time but at different rates in the order: free DOX > Chol-SS-COS/DOX-L > Chol-COS/DOX-L for both cells. DOX dosage was 20 $\mu$g/ml for all cases but the uptake of the two liposome formulations by MG63 was significantly different. * $p < 0.05$ and ** $p < 0.01$. Data are mean ± SD ($n = 3$).

chitooligosaccharides (COS) (MW 2000-5000), a hydrolytic product of chitosan, on the surface via a disulfide bond was designed to unite the three targeting features (Scheme 1).

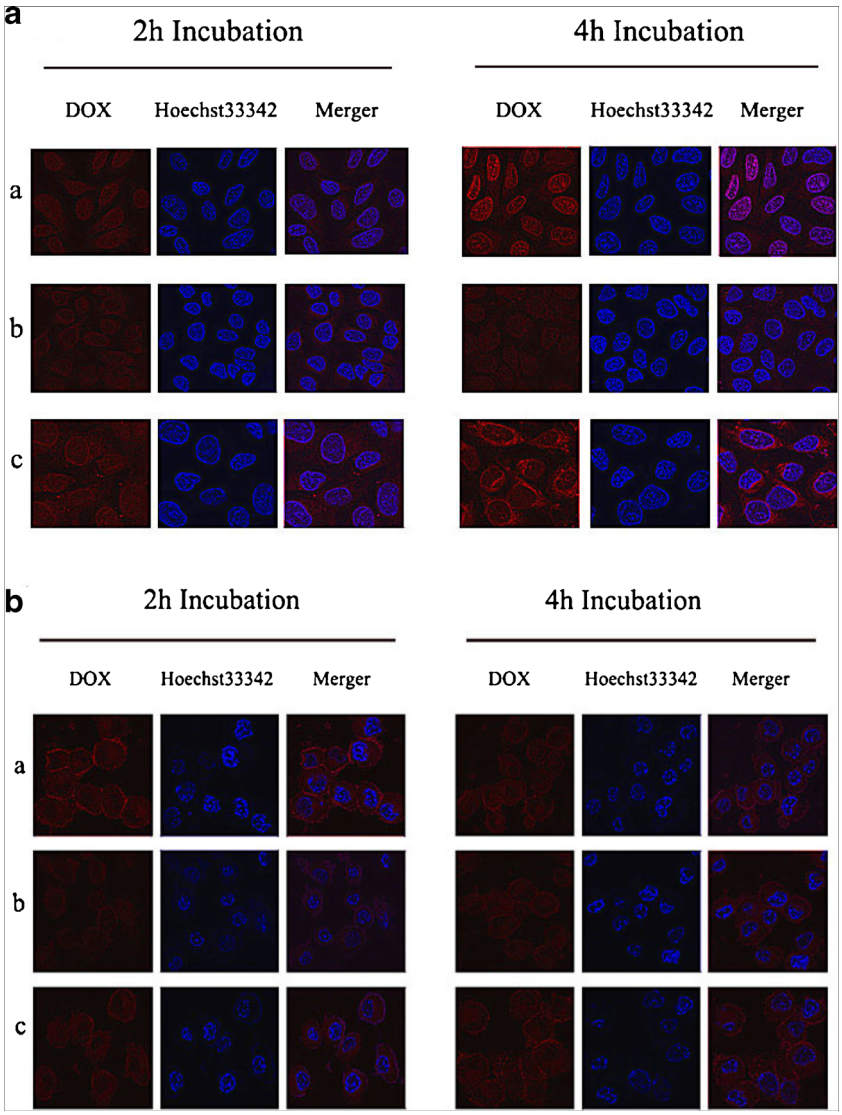


**Fig. 7** Confocal microscopy images of (**A**) MG63 cells and (**B**) LO2 cells. Cells were treated with free DOX (**a**), Chol-COS/DOX-L (**b**), Chol-SS-COS/DOX-L (**c**) incubated for 2 h and 4 h, respectively, for both cases. Red: DOX; Blue: nuclear staining with Hoechst dye.

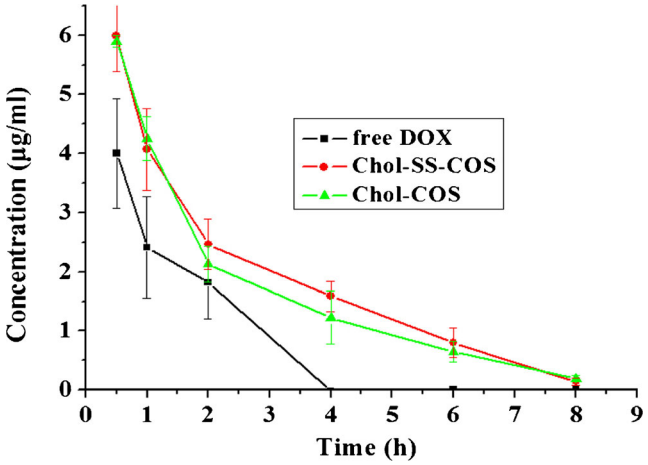


**Fig. 8** Mean plasma DOX concentration-time profiles following intravenous injection of the DOX liposomes or a DOX solution to rats at a dose of 2 mg/kg. Data are mean ± SD ($n$ = 3).

To enable construction of the liposomes, a novel cholesterol derivative, Chol-SS-CCOH, was first synthesized and its structure was confirmed with NMR. The successful conjugation of COS with Chol-SS-COOH pre-inserted in the liposome bilayer was verified with FTIR (Fig. 1), and also evidenced by the increases in size and zeta potential (from negative to positive values) of both resulted liposomes (Table I). However, due to the lack for quantitative assay the conjugation efficiency of COS on the liposomes were not determined. The stable Chol-SS-COS/DOX liposomes with a high drug loading of DOX had a size of 105 nm, close to Doxil®. The liposomes were cationic with zeta potential values of 34-37 mV, which is higher than N-palmitoyl chitosan anchored liposomes (20 mV) [20] or glycol-chitosan modified liposomes [25]. In contrast to glycol-chitosan coated liposomes which demonstrated a pH-dependent zeta potential (+10 mV at pH 6, −15 mV at pH 7.4) [25], there was no obvious change in zeta potential over pH 6 - 7.4 with the COS modified liposomes. This can be attributed to the higher density of -$NH_2$ groups resulted from high degree of de-acetylation (75%) of COS, which are positively charged within the pH range.

Cationic liposomes have shown to selectively target tumor endothelial cells with a preferential uptake in angiogenic tumor vessels [31, 32]. Furthermore, the cellular uptake of liposomes is generally believed to be mediated by adsorption of liposomes onto the cell surface, subsequently facilitating endocytosis [33]. It is well documented that the surface of cancer cells are negatively charged due to secretion of a large amount of lactate anions across membranes, whereas the surfaces of normal cells remain charge-neutral or slightly positive [34]. Therefore, positively charged liposomes can selectively interact with cancer cells and facilitate cellular uptake via endocytosis [25, 33]. This was also observed with Chol-SS-COS/DOX-L and the non-reduction sensitive Chol-COS/DOX-L in this study.

Chol-SS-COS/DOX-L was stable in PBS (pH 7.4) containing 10% FBS (Fig. 3) and exhibited a sustained drug release property at pH 7.4 in the absence of GSH (Fig. 4). This suggested the good drug retention in the liposomes with minimal leakage during blood circulation. Drug leakage *in vivo* is often a major challenge in liposomes development [35] while crucial to achieve EPR effect [36]. Further, the *in vitro* study indicated that Chol-SS-COS-L were reduction-sensitive, evidenced by the destabilization of the liposome structure in reducing agent DTT, most likely due to disulfide bond breakage (Fig. 3). The cleavage of COS might have resulted in fusion of liposomes given the samples looked more 'milky'. However, it is unknown how much of the COS was cleaved off. Further study showed that the drug release from Chol-SS-COS/DOX-L could be sufficiently trigged by the presence of GSH at the tumoral intracellular concentration (10 mM),

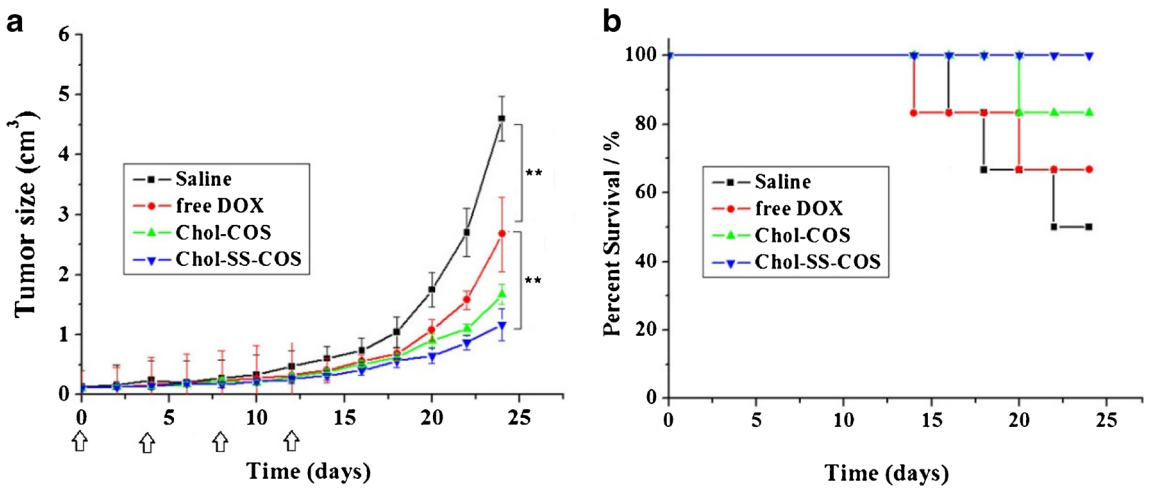


**Fig. 9** Tumor growth curves (**A**) and survival rates (**B**) of MG63 tumor-bearing mice following i.v. injection of different DOX formulations. The treatment started on Day 0 (when the tumor volume reached 100 $mm^3$) and was repeated on Day 4, 8 and 12 at a dose of 5 mg/kg. Data in (A) are mean ± SD ($n$ = 6 or less as a result of animal death). **p<0.01.

but not the extracellular level (20 μM) (Fig. 4). Figure 4 also shows that Chol-COS/DOX-L also gave slightly higher drug release in the first a few hours in response to addition of 10 mM GSH to PBS, possibly due to the higher osmotic pressure of the release medium.

MTT assay of COS polymer and COS modified liposomes showed good biocompatibility with cells (Fig. 5A). Different form Chol-COS/DOX-L, Chol-SS-COS/DOX-L was demonstrated to more cytotoxic to MG63 cells, but no difference to LO2 (Table II). A few reasons can explain this selective cytotoxicity: 1) the charge effect on the two different cells with MG63 surface being more negatively charged than LO2 resulting in enhanced cellular uptake of the cationic liposomes, and 2) the higher concentration of GSH in cancer cells MG63 than normal cells. The intracellular cleavage of -SS- bond by GSH resulted in detachment of COS from liposomes, and subsequent destabilization of liposomes, promoting endosome escape into the cell cytoplasm [3]. In addition, compared with free DOX, the $IC_{50}$ of Chol-SS-COS/DOX-L was higher which reflects the different cellular uptake mechanisms and sustained release from liposomes. Nanocarriers entered tumor cells via endocytosis, which may be slower than diffusion of free DOX. However, *in vitro* cytotoxicity tests do not always reflect the *in vivo* circumstances such as the EPR effect. In the body, free DOX will be widely distributed into tissues with only a small amount reaching tumor cells.

Cellular uptake by MG63 and LO2 cells was quantified using flow cytometry, and confocal microscopy, the formations were ranked as DOX > Chol-SS-COS/DOX-L > Chol-COS/DOX-L. This is consistent with the cytotoxicity data. The significant improvement of Chol-SS-COS/DOX-L over Chol-COS/DOX-L demonstrated the crucial roles of the intracellular detachment of COS in the bioavailability of DOX and the cytotoxic effects. Confocal images of Chol-COS/DOX-L treated MG63 showed some small dots, indicating the internalized liposomes might have been entrapped inside endosome-lysosomal vesicles. It was also noted that DOX formulations, particularly Chol-SS-COS/DOX-L, produced stronger fluorescence intensity in MG63 cells than LO2. This may be due to the more significant negative charge of cancer cells than normal cells which not only enhanced the cellar uptake of cationic liposomes but also attracted the cationic DOX (basic $pK_a$ 8.4).

**Table II** Pharmacokinetic parameters of DOX following intravenous injection of DOX solution or liposomes at a dose of 2 mg/kg to rats. Data present as mean ± SD ($n$ = 3)

| Parameter | Free DOX | Chol-SS-COS/DOX | Chol-COS/DOX |
|---|---|---|---|
| $C_{max}$ (μg/ml) | 4.00 ± 0.93 | 5.99 ± 0.60 | 5.89 ± 0.10 |
| AUC (μg /ml·h) | 6.5 ± 1.1 | 17.8 ± 1.2 | 14.8 ± 2.1 |
| $T_{1/2}$ (min) | 16.8 ± 0.4 | 68.0 ± 9.1 | 93.4 ± 16.9 |
| MRT (min) | 62.1 ± 13.8 | 148.2 ± 13.6 | 165.4 ± 13.1 |

Long circulation property of nanocarriers is critical for passive tumor targeting through the potential EPR effect [11]. Following i.v. injection to rats at a dose of 2 mg/kg, the Chol-SS-COS/DOX-L and Chol-COS/DOX-L resulted in approximately 3-fold increase in AUC, and 4.0 and 5.5-fold increases in the elimination $T_{1/2}$, compared to DOX solution (Fig. 8 and Table II). The relatively shorter $T_{1/2}$ of Chol-SS-COS/DOX than Chol-COS/DOX may partially be caused by the faster DOX release (Figure 4) [36] and partially due to the positive charge which led to non-specific interactions with anionic proteins in the blood and subsequent clearance by the RES [12]. Additionally, a study in tumor-bearing mice by Gabizon *et al.* [37] using PEGylated liposome of DOX (Doxil) at doses ranging 2.5-20 mg/kg demonstrated that the liposomes clearance by the RES system is a saturated process, with lower dose being cleared disproportional faster. However, in this study the drug concentration was measurable even at 48 h post injection of Doxil at all dose elvels. Therefore, longer circulation may be expected should the dose was increased for the COS-coated liposomes, however, long-circulation property of COS-coating did not appear to be as effective as PEGylation. Another note is that redox-responsive liposomes with detachable PEG coating via disulfide bond were previously developed [38, 39] but pharmacokinetic studies suggested that PEG layer was rapidly cleaved in circulation [39]. To our best knowledge, this paper is the first study using chitooligosaccharides (COS) to modify liposomal surface, and the coating through disulfide bond was GSH-sensitive and stable in blood circulation.

After four i.v. in the MG63 tumor-bearing nude mice at a DOX dose of 5 mg/kg *both liposomes* resulted in not only significantly enhanced inhibitory effect on tumor growth than the free DOX, but also the survival rate of animals (Fig. 9). Compared with Chol-COS/DOX-L, the GSH-sensitive liposomes, Chol-SS-COS/DOX-L was more efficient in tumor suppression, due to accelerated release of DOX from cytoplasmic by GSH-induced cleavage of -SS- bonds. These results also indicated that the inexpensive polymer COS had good biocompatibility, and may be a promising alternative polymer to PEG for stabilization of liposomes, evidenced from the high survival rate of animals. The 20% death ($n$ = 1) from Chol-COS/DOX-L was likely due to the tumor growth effect.

## CONCLUSIONS

Conjugation of liposomes with chitooligosaccharides (COS) (MW 2000-5000) extended the liposomal blood circulation time and enhanced the efficiency of intracellular delivery, thus

**improved the anti-tumor efficacy and animal survival rate.**

COS may be a promising polymer to stabilize liposomes with an advantages of enhanced cellular uptake, c**ost-effective and possibly good biocompatibility**. This study also highlighted the importance of intracellular 'detachment' of polymer from liposomes through the cleavage of the disulfide bond in cytoplasmic drug delivery. Taken together, the reduction (GSH)-sensitive Chol-SS-COS liposomes may be excellent platform for cytoplasmic drug delivery to tumor such as osteosarcomas.

*ACKNOWLEDGMENTS AND DISCLOSURES*. This study was financially supported by Taishan Scholar Project carried out at School of Pharmacy, Yantai University, funded by Shandong Province, China. The authors declare that they have no conflicts of interest to disclose.

## REFERENCES

1. Jain A, Jain SK. Stimuli-responsive smart liposomes in cancer targeting. Curr Drug Targets. 2016.
2. Jhaveri A, Deshpande P, Torchilin V. Stimuli-sensitive nanopreparations for combination cancer therapy. J Control Release. 2014;190:352–70.
3. Torchilin VP. Multifunctional, stimuli-sensitive nanoparticulate systems for drug delivery. Nat Rev Drug Discov. 2014;13(11):813–27.
4. Maeda H. The enhanced permeability and retention (EPR) effect in tumor vasculature: the key role of tumor-selective macromolecular drug targeting. Adv Enzym Regul. 2001;41:189–207.
5. Kuppusamy P, Li H, Ilangovan G, Cardounel AJ, Zweier JL, Yamada K, et al. Noninvasive imaging of tumor redox status and its modification by tissue glutathione levels. Cancer Res. 2002;62(1):307–12.
6. Zhou G, Li L, Xing J, Jalde S, Li Y, Cai J, et al. Redox responsive liposomal nanohybrid cerasomes for intracellular drug delivery. Colloids Surf B Biointerfaces. 2016;148:518–25.
7. Latorre A, Somoza A. Glutathione-triggered drug release from nanostructures. Curr Top Med Chem. 2014;14(23):2662–71.
8. Felber AE, Dufresne MH, Leroux JC. pH-sensitive vesicles, polymeric micelles, and nanospheres prepared with polycarboxylates. Adv Drug Deliv Rev. 2012;64(11):979–92.
9. Kanamala M, Wilson WR, Yang M, Palmer BD, Wu Z. Mechanisms and biomaterials in pH-responsive tumour targeted drug delivery: A review. Biomaterials. 2016;85:152–67.
10. Zhu L, Kate P, Torchilin VP. Matrix metalloprotease 2-responsive multifunctional liposomal nanocarrier for enhanced tumor targeting. ACS Nano. 2012;6(4):3491–8.
11. Maruyama K. Intracellular targeting delivery of liposomal drugs to solid tumors based on EPR effects. Adv Drug Deliv Rev. 2011;63(3):161–9.
12. Torchilin V. Multifunctional and stimuli-sensitive pharmaceutical nanocarriers. Eur J Pharm Biopharm. 2009;71(3):431–44.
13. Moghimi SM, Hunter AC, Murray JC. Long-circulating and target-specific nanoparticles: theory to practice. Pharmacol Rev. 2001;53(2):283–318.
14. Kiibanov AL, Huang L. Long-Circulating Liposomes: Development and Perspectives. J Liposome Res. 1992;2(3):321–34.
15. Hatakeyama H, Ito E, Akita H, Oishi M, Nagasaki Y, Futaki S, et al. A pH-sensitive fusogenic peptide facilitates endosomal escape and greatly enhances the gene silencing of siRNA-containing nanoparticles in vitro and in vivo. J Control Release. 2009;139(2):127–32.
16. Remaut K, Lucas B, Braeckmans K, Demeester J, De Smedt SC. Pegylation of liposomes favours the endosomal degradation of the delivered phosphodiester oligonucleotides. J Control Release. 2007;117(2):256–66.
17. Ishida T, Kiwada H. Accelerated blood clearance (ABC) phenomenon upon repeated injection of PEGylated liposomes. Int J Pharm. 2008;354(1-2):56–62.
18. Kierstead PH, Okochi H, Venditto VJ, Chuong TC, Kivimae S, Frechet JM, et al. The effect of polymer backbone chemistry on the induction of the accelerated blood clearance in polymer modified liposomes. J Control Release. 2015;213:1–9.
19. Qu G, Wu X, Yin L, Zhang C. N-octyl-O-sulfate chitosan-modified liposomes for delivery of docetaxel: preparation, characterization, and pharmacokinetics. Biomed Pharmacother. 2012;66(1):46–51.
20. Liang G, Jia-Bi Z, Fei X, Bin N. Preparation, characterization and pharmacokinetics of N-palmitoyl chitosan anchored docetaxel liposomes. J Pharm Pharmacol. 2007;59(5):661–7.
21. Lee SJ, Min HS, Ku SH, Son S, Kwon IC, Kim SH, et al. Tumor-targeting glycol chitosan nanoparticles as a platform delivery carrier in cancer diagnosis and therapy. Nanomedicine. 2014;9(11):1697–713.
22. Yang Y, Yuan SX, Zhao LH, Wang C, Ni JS, Wang ZG, et al. Ligand-directed stearic acid grafted chitosan micelles to increase therapeutic efficacy in hepatic cancer. Mol Pharm. 2015;12(2):644–52.
23. Huo M, Zhang Y, Zhou J, Zou A, Yu D, Wu Y, et al. Synthesis and characterization of low-toxic amphiphilic chitosan derivatives and their application as micelle carrier for antitumor drug. Int J Pharm. 2010;394(1-2):162–73.
24. Liu Z, Jiao Y, Wang Y, Zhou C, Zhang Z. Polysaccharides-based nanoparticles as drug delivery systems. Adv Drug Deliv Rev. 2008;60(15):1650–62.
25. Yan L, Crayton SH, Thawani JP, Amirshaghaghi A, Tsourkas A, Cheng Z. A pH-responsive drug-delivery platform based on glycol chitosan-coated liposomes. Small. 2015;11(37):4870–4.
26. Lodhi G, Kim YS. Chitooligosaccharide and its derivatives: preparation and biological applications. 2014. ID: 654913.
27. Muanprasat C, Chatsudthipong V. Chitosan oligosaccharide: Biological activities and potential therapeutic applications. Pharmacol Ther. 2016;170:80–97.
28. Zou P, Yang X, Wang J, Li Y, Yu H, Zhang Y, et al. Advances in characterisation and biological activities of chitosan and chitosan oligosaccharides. Food Chem. 2016;190:1174–81.
29. Mendis E, Kim MM, Rajapakse N, Kim SK. An in vitro cellular analysis of the radical scavenging efficacy of chitooligosaccharides. Life Sci. 2007;80(23):2118–27.
30. Yu J-M, Li Y-J, Qiu L-Y, Jin Y. Self-aggregated nanoparticles of cholesterol-modified glycol chitosan conjugate: Preparation, characterization, and preliminary assessment as a new drug delivery carrier. Eur Polym J. 2008;44(3):555–65.
31. Wu J, Lee A, Lu Y, Lee RJ. Vascular targeting of doxorubicin using cationic liposomes. Int J Pharm. 2007;337(1-2):329–35.
32. Abu Lila AS, Ishida T, Kiwada H. Targeting anticancer drugs to tumor vasculature using cationic liposomes. Pharm Res. 2010;27(7):1171–83.
33. Miller CR, Bondurant B, McLean SD, McGovern KA, O'Brien DF. Liposome-cell interactions in vitro: effect of liposome surface

charge on the binding and endocytosis of conventional and sterically stabilized liposomes. Biochemistry. 1998;37(37):12875–83.
34. Chen B, Le W, Wang Y, Li Z, Wang D, Ren L, et al. Targeting Negative Surface Charges of Cancer Cells by Multifunctional Nanoprobes. Theranostics. 2016;6(11):1887–98.
35. Zhang W, Falconer JR, Baguley BC, Shaw JP, Kanamala M, Xu H, et al. Improving drug retention in liposomes by aging with the aid of glucose. Int J Pharm. 2016;505(1-2):194–203.
36. Wang X, Song Y, Su Y, Tian Q, Li B, Quan J, et al. Are PEGylated liposomes better than conventional liposomes? A special case for vincristine. Drug Deliv. 2016;23(4):1092–100.
37. Gabizon A, Tzemach D, Mak L, Bronstein M, Horowitz AT. Dose dependency of pharmacokinetics and therapeutic efficacy of pegylated liposomal doxorubicin (DOXIL) in murine models. J Drug Target. 2002;10(7):539–48.
38. Kirpotin D, Hong K, Mullah N, Papahadjopoulos D, Zalipsky S. Liposomes with detachable polymer coating: destabilization and fusion of dioleoylphosphatidylethanolamine vesicles triggered by cleavage of surface-grafted poly(ethylene glycol). FEBS Lett. 1996;388(2-3):115–8.
39. Ishida T, Kirchmeier MJ, Moase EH, Zalipsky S, Allen TM. Targeted delivery and triggered release of liposomal doxorubicin enhances cytotoxicity against human B lymphoma cells. Biochim Biophys Acta. 2001;1515(2):144–58.